

## Original Article

# Usefulness of dynamic contrast-enhanced magnetic resonance imaging for predicting treatment response to vinorelbine-cisplatin with or without recombinant human endostatin in bone metastasis of non-small cell lung cancer

Rui Zhang<sup>1\*</sup>, Zhi-Yu Wang<sup>1\*</sup>, Yue-Hua Li<sup>2</sup>, Yao-Hong Lu<sup>3</sup>, Shuai Wang<sup>4</sup>, Wen-Xi Yu<sup>1</sup>, Hui Zhao<sup>1</sup>

Departments of <sup>1</sup>Internal Oncology, <sup>2</sup>Radiology, <sup>3</sup>Clinical Skill Laboratory, Shanghai Sixth People's Hospital Affiliated to Shanghai Jiaotong University, Shanghai 200233, People's Republic of China; <sup>4</sup>Department of Internal Oncology, Shanghai Sixth People's Hospital, Soochow University, Shanghai 200233, People's Republic of China. \*Equal contributors.

Received October 11, 2016; Accepted November 8, 2016; Epub December 1, 2016; Published December 15, 2016

**Abstract:** Metastatic bone disease is a frequent complication of advanced non-small cell lung cancer (NSCLC) and causes skeletal-related events, which result in a poor prognosis. Currently, no standard method has been developed to precisely assess the therapeutic response of bone metastases (BM) and the early efficacy of anti-angiogenic therapy, which does not conform to the concept of precision medicine. This study aimed to investigate the usefulness of dynamic contrast-enhanced magnetic resonance imaging (DCE-MRI) for precise evaluation of the response to chemotherapy with anti-angiogenic agents in NSCLC patients with BM. Patients were randomly assigned to a treatment group (vinorelbine + cisplatin [NP] + recombinant human endostatin [rh-endostatin]) or a control group (NP + placebo). All patients were evaluated before treatment and after 2 cycles of treatment using DCE-MRI quantitative analysis technology for BM lesions and chest computed tomography (CT). Correlations between changes in the DCE-MRI quantitative parameters and treatment effect were analyzed. We enrolled 33 patients, of whom 28 were evaluable (20 in the treatment group and 8 in the control group). The results suggested a higher objective response rate (30% vs. 0%), better overall survival ( $21.44 \pm 17.28$  months vs.  $7.71 \pm 4.68$  months), and a greater decrease in the transport constant (Ktrans) value (60% vs. 4.4%) in the treatment group than in the control group ( $P < 0.05$ ). The Ktrans values in the "partial remission plus stable disease (PR + SD)" group were significantly lower after treatment ( $P < 0.05$ ). Patients with a decrease of  $> 50\%$  in the Ktrans value showed a significantly better overall survival than those with a decrease of  $\leq 50\%$  (13.2 vs. 9.8 months,  $P < 0.05$ ). Ktrans as a DEC-MRI quantitative parameter could be used for the precise evaluation of BM lesions after anti-angiogenic therapy and as a predictor of survival. In addition, we reconfirmed the anti-angiogenic effect of rh-endostatin in NSCLC patients with BM.

**Keywords:** DCE-MRI, quantitative parameters, non-small cell lung cancer, bone metastases, anti-angiogenic therapy, recombinant human endostatin, therapeutic response

## Introduction

Lung cancer is one of the most common malignant tumors, with non-small cell lung cancer (NSCLC) accounting for about 85% of all cases [1, 2]. The incidence of bone metastases (BM) in advanced NSCLC is estimated to range from 30% to 40% [3]. Fifty percent of patients with BM are vulnerable to skeletal-related events, including severe bone pain, pathological frac-

tures, spinal cord compression, and hypercalcemia, which could lead to a shorter survival time [4].

According to the World Health Organization (WHO) criteria, BM are non-measurable lesions [5]. In the recently revised Response Evaluation Criteria in Solid Tumors (RECIST) guidelines (version 1.1), osteolytic or mixed lesions with identifiable soft tissue components are consid-

ered measurable lesions using computed tomography (CT) and magnetic resonance imaging (MRI). In contrast, osteoblastic lesions are still considered non-measurable [6].

Currently, the precision medicine concept is widely used in oncology research, and targeted therapy for lung cancer belongs to this category [7]. The main targeted therapy for lung cancer includes the use of inhibitors of epidermal growth factor receptor (EGFR), vascular endothelial growth factor (VEGF), and other targets identified recently [8, 9]. Anti-angiogenic therapy is a major research focus in the treatment of NSCLC. It is based on the theory that tumor growth over a certain volume needs a functional vascular system [10]. Endostar is a new recombinant human endostatin (rh-endostatin) developed by Chinese researchers that could specifically inhibit the proliferation of vascular endothelial cells and tumor growth by interfering with normal cell signaling pathways or improving the sensitivity of tumor cells to other treatments [11]. Rh-endostatin directly targets new capillary endothelial cells around the tumor, although it may not induce a significant decrease in tumor volume; this leads to the phenomenon in which the tumor volume changes later than the suppression of its blood supply [12-14].

Precision medicine includes not only precision treatment but also accurate estimation of therapeutic effects [15]. In clinical practice, it is difficult to precisely evaluate the therapeutic response of BM lesions and the early efficacy of anti-angiogenic therapy. Thus, we applied dynamic contrast-enhanced MRI (DCE-MRI) quantitative analysis technology to achieve this goal. DCE-MRI involves repeated imaging of the distribution of an intravenous contrast agent, which can be used to measure properties of the tissue microvasculature [16, 17]. DCE-MRI could provide vascular functional quantitative parameters, such as the transport constant ( $K_{trans}$ ), rate constant ( $K_{ep}$ ), and extravascular extracellular volume fraction ( $V_e$ ) using a two-compartment model, which can be used to evaluate the physiological characteristics of tumor blood vessels [18, 19]. Thus, DCE-MRI technology contributes to the establishment of objective criteria for the diagnosis and assessment of therapeutic effects. In this study, we used DCE-MRI quantitative analysis to assess the therapeutic response and early efficacy of

anti-angiogenic therapy in NSCLC patients with BM.

### Patients and methods

#### *Study design*

This phase IV, randomized, open, prospective, double-blind, placebo-controlled study was approved by the medical ethics committee of the head unit of Shanghai Jiaotong University Affiliated Sixth People's Hospital. The clinical trial was approved by the China State Food and Drug Administration. China Clinical Trials Registry No. chictr-ctr-09000569, October 22, 2009.

#### *Inclusion criteria*

Subjects included in this study were NSCLC patients who: (1) had BM confirmed using pathological or cytological examinations; (2) had imaging data that showed pelvic metastatic lesions; (3) were aged 18 to 75 years; (4) had an expected survival time of  $\geq 3$  months; (5) did not receive taxane, bevacizumab, thalidomide, rh-endostatin, or bisphosphonate therapy, and evaluable BM were not treated with radiotherapy for 3 months before the study; (6) had normal routine blood examination results, liver and kidney function, and electrocardiogram results; (7) had no evidence of cardiovascular diseases, autoimmune diseases, vasculitis, severe infections, diabetes, or other concomitant diseases; and (8) gave their informed consent.

#### *Exclusion criteria*

Patients who (1) received granulocyte colony-stimulating factor or granulocyte-macrophage colony-stimulating factor (GM-CSF) during chemotherapy; (2) could not tolerate adverse reactions; and (3) were allergic to contrast agents were excluded from the study.

#### *Endpoints*

The primary endpoints were objective response rate (ORR) and disease control rate (DCR). The secondary endpoints included overall survival (OS) and progression-free survival (PFS). The exploratory endpoints were DCE-MRI quantitative parameters ( $K_{trans}$ ,  $K_{ep}$ , and  $V_e$ ), bone metabolism markers, tumor markers, and angiogenesis-related genes.

### *Random assignment and blinding*

The patients were randomly assigned to the treatment or control groups at a ratio of 2:1, in a double-blind fashion. Codes were generated via a randomization method by an independent biostatistician. According to these random codes, therapeutic agents were numbered by a nurse who was not involved in the trial. Patients were enrolled in this program, and agents were distributed in sequence. The trial sponsor, investigators, and patients were blinded to the treatment assignment.

### *Treatment*

Vinorelbine and cisplatin were obtained from the Pierre Fabre pharmaceutical company and Qilu Pharmaceutical Limited, respectively. Vinorelbine (25 mg/m<sup>2</sup> on days 1 and 8) and cisplatin (75 mg/m<sup>2</sup> on day 1) were administered. The rh-endostatin injection was obtained from Shandong Simcere-Medgenn Bio-Pharmaceuticals. The placebo was normal saline. The patients received rh-endostatin (7.5 mg/m<sup>2</sup>/day) or a placebo from days 1 to 14 of every cycle. Rh-endostatin was dissolved in 250 mL of normal saline and administered through intravenous infusion for at least 3 hours. The patients in both groups received 4 cycles of treatment. If intolerable adverse events occurred, treatment was terminated. All patients underwent an initial chest CT scan, DCE-MRI of the pelvis, and blood sampling before treatment and after 2 cycles of treatment. After 2 cycles of chemotherapy, the patients were followed up once a month for the first 3 months, then once every 3 months, and 1 year after that they were followed up once every 6 months. The follow-up examination included the following: routine blood analysis, liver and kidney function, electrolytes, blood calcium level, tumor markers, bone metabolites, and chest CT. The follow-up continued until disease progression or death.

### *Pelvic DCE-MRI*

All patients were evaluated twice using DCE-MRI. The first evaluation was performed within 1 week before treatment, and the second evaluation was performed within 1 week after completion of 2 cycles of treatment. All MRI exami-

nations were performed at Shanghai Sixth People's Hospital using the 3.0-T Siemens Magnetom Avanto System (Siemens Healthcare, Erlangen, Germany) with a pelvic multi-channel phased-array coil. Non-enhanced fast-recovery fast-spin echo T1-weighted images (FSE T1WIs) were obtained on the axial, sagittal, and coronal planes (repetition time, 650-800 ms; echo time, 7-10 ms; slice thickness, 5-8 mm/gap; field of view, 18-36 cm; acquisition matrix, 256 × 192; number of excitations [NEX], 2; and flip angle, 40°), which covered the entire pelvis. Axial, sagittal, and coronal fast-recovery fast-spin echo T2-weighted images (FSE T2WIs) were obtained using the following parameters: (repetition time, 4000-5000 ms; echo time, 80-100 ms; slice thickness, 5-8 mm/gap; field of view, 18-36 cm; acquisition matrix, 320 × 224; NEX, 2; flip angle, 40°). DCE-MRIs were acquired after intravenous injection of gadolinium-diethylenetriamine penta-acetic acid (Magnevist, Schering, Berlin, Germany) at a dose of 0.1 mmol/kg of body weight and a rate of 2 mL/s, followed by subsequent washing with 20 mL brine at the same speed. Using a transverse three-dimensional T1-weighted spoiled gradient-echo sequence (repetition time, 4.1-5.6 ms; echo time, 1.2-1.4 ms; slice thickness, 5-8 mm/gap; field of view, 24 cm; acquisition matrix, 256 × 192; NEX, 1; and flip angle, 20°).

### *Image analysis*

The acquired MR images were analyzed by one experienced radiologist who was blinded to the patients' treatment response and all clinical data except the patients' name, sex, and age. A two-compartment model was used to analyze the images to evaluate perfusion and vascular permeability of pelvic metastases. Quantitative parameters, such as K<sub>trans</sub>, K<sub>ep</sub>, and V<sub>e</sub>, can be derived from this model as imaging indicators. Regions of interest (ROI), which excluded non-enhancing tissue, were drawn around the whole lesion on the slice that demonstrated the greatest contrast uptake (ROI<sub>whole</sub>) [20]. For each patient, an experienced radiologist manually selected the ROI on the pelvic metastatic lesion on the DCE-MRI scans in order to guarantee that the patients' ROI were the same size before and after treatment. The ROI on the remaining image can then be automatically calibrated for maximum relevance.

## DCE-MRI in the prediction of endostatin effect in NSCLC patients with BM

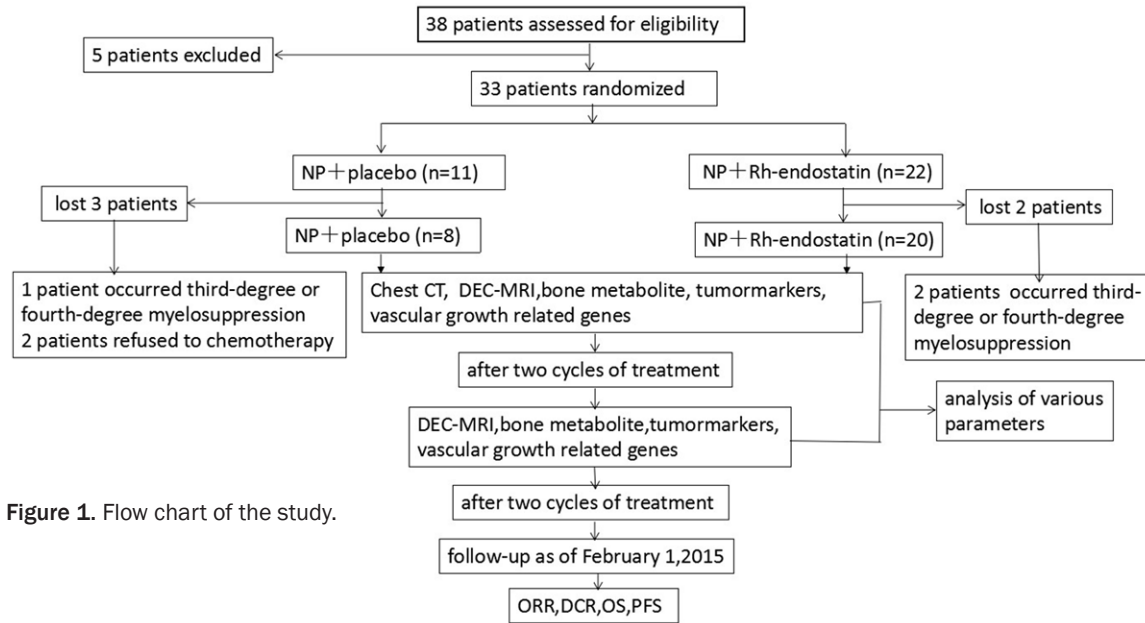


**Figure 1.** Flow chart of the study.

**Table 1.** Baseline characteristics for all patients enrolled in the trial

Characteristic	NP + rh-endostatin (N = 20)	NP + Placebo (N = 8)	<i>p</i> value
Sex			0.55
Male	9	4	
Female	11	4	
Age			0.80
Median ± SD	59.78 ± 4.73	61.29 ± 9.74	
Pathologic type			0.45
Adenocarcinoma	11	4	
Squamous cell carcinoma	2	2	
Poor differentiated carcinoma	7	2	
Character of BM			0.72
Lytic	10	4	
Blastic	2	1	
Mixed	8	3	
With visceral metastases			0.48
Yes	9	4	
No	11	4	

*P* > 0.05.

### Statistical analyses

All the statistical analyses were performed using SPSS version 21.0 (SPSS Inc., Chicago, IL, USA). *P* values of 0.05 were considered statistically significant. Data are expressed as mean ± standard deviation. Ktrans, Kep, Ve, bone metabolites, tumor markers, and tumor

vascular growth-related factors before and after treatments were compared using a paired *t*-test. Kaplan-Meier survival analysis was used to determine the correlation between selected parameters and PFS or OS. The difference in Ktrans between the “partial remission plus stable disease (PR + SD)” group and the disease progression (PD) group was tested using a chi-square test.

### Results

#### Patient characteristics

From January 1, 2009, to February 1, 2011, 33 patients with BM of advanced NSCLC were enrolled in this study and randomly assigned to the treatment (n = 22) or control

groups (n = 11). After the first treatment cycle, 2 patients in the treatment group and 1 patient in the control group who had third- or fourth-degree myelosuppression received GM-CSF. Two patients in the control group refused GM-CSF treatment. Three patients were excluded from the study because GM-CSF administration could promote the formation of new blood

**Table 2.** Treatment response evaluation in the two groups

	Response Evaluation				Total N
	CR N (%)	PR N (%)	SD N (%)	PD N (%)	
NP + Rh-endostatin	0 (0%)	6 (30%)	10 (50%)	4 (20%)	20
NP + Placebo	0 (0%)	0 (0%)	6 (75%)	2 (25%)	8

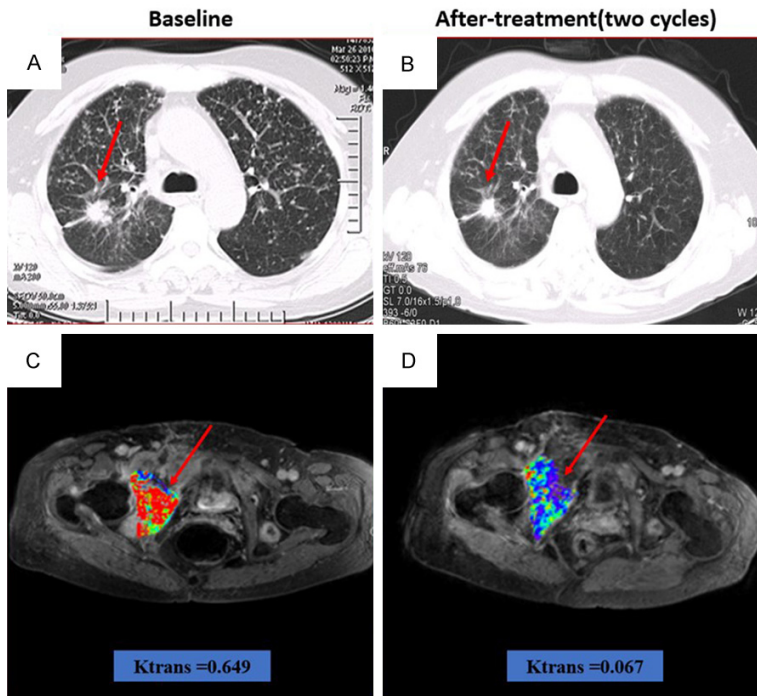


**Figure 2.** This is a male patient aged 60 with lung adenocarcinoma. A: Lung lesions before treatment. B: After 2 cycles of treatment (NP + rh-endostatin), the volume of lung lesion decreased significantly. C: Ktrans before treatment was 0.649. D: After 2 cycles of treatment Ktrans dropped to 0.067.

vessels in vivo. GM-CSF administration could have an impact on our results. This view has been confirmed by in vitro studies [21, 22], although these studies are relatively rare. In the efficacy analysis, 28 cases in the treatment (n = 20) and control groups (n = 8) were included. The basic clinical parameters were not significantly different between the 2 groups, which showed good uniformity at baseline. In the treatment group, 7 patients completed 2 cycles of chemotherapy and 13 patients completed 4 cycles. The study procedure is shown in **Figure 1**. Data regarding patient characteristics are shown in **Table 1**.

*Primary endpoints*

In the treatment group, 6 patients (30%) achieved PR; 10 (50%) achieved SD; and 4

(20%) experienced PD. The PR, SD, and PD rates in the control group were 0%, 75%, and 25%, respectively. The ORR in the treatment group was 30% (6/18) compared with 0% in the control group (P < 0.001). The DCRs were 80% and 75% in the treatment and control groups, respectively (P > 0.05; **Table 2**). After 2 treatment cycles, 1 patient underwent chest CT and DEC-MRI; the quantitative analysis images of the pelvic metastatic lesions showed PD in the efficacy evaluation (**Figure 2**).

*Secondary endpoints*

After a median follow-up of 33.8 months, the mean PFS times were 6.55 ± 2.93 and 5.28 ± 2.28 months (P > 0.05) in the treatment and control groups (**Figure 3A**), respectively, and the OS times were 21.44 ± 17.28 months and 7.71 ± 4.68 months (P = 0.008; **Figure 3B**), respectively. The OS in the treatment group was longer than that in the control group.

*Exploratory endpoints*

Quantitative analysis of DCE-MRI data revealed that Ktrans decreased from 0.60 ± 0.94/min at baseline to 0.24 ± 0.43/min (P = 0.02) in the treatment group, and from 2.51 ± 5.55/min to 2.40 ± 5.02/min (P > 0.05) in the control group. The decrease in Ktrans value in the treatment group was significantly greater than that in the control group. The other parameters, including Kep, Ve, bone metabolism, tumor markers, and angiogenesis-related genes, were not significantly different between the 2 groups before and after treatment (**Table 3**).

Further analysis of the data in comparison with that at baseline showed that patients with a decrease of > 50% in the Ktrans value showed a significantly longer OS (13.2 vs. 9.8 months)

## DCE-MRI in the prediction of endostatin effect in NSCLC patients with BM

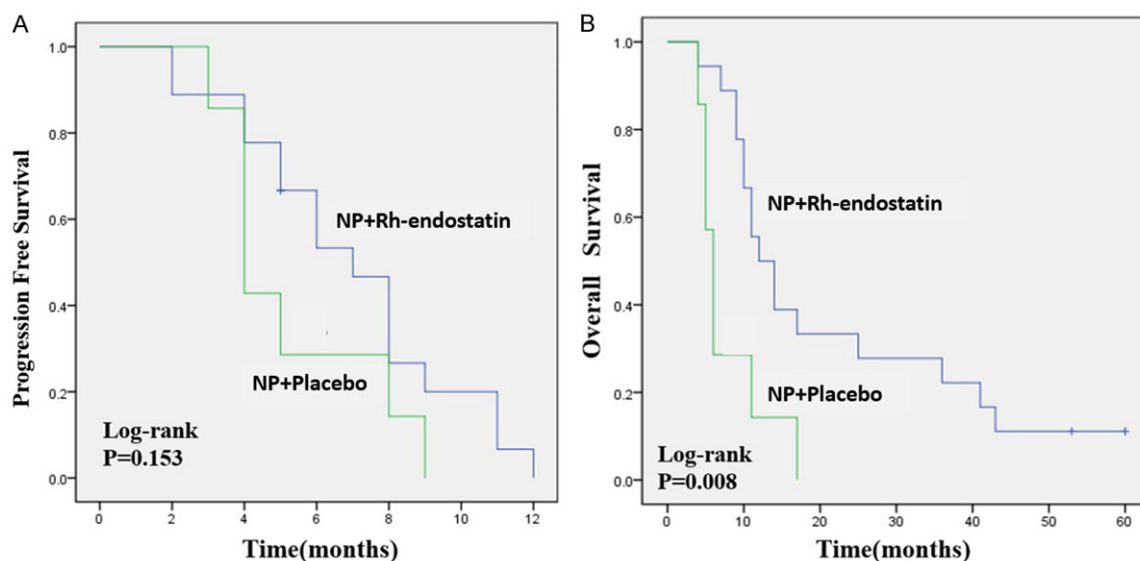


**Figure 3.** PFS and OS in the two groups. A: The PFS between the two groups was not significantly different ( $P = 0.153$ ). B: The OS was significantly different in the two groups ( $P = 0.008$ ).

**Table 3.** Various parameters change of two groups before and after treatment

			Before treatment	After treatment	<i>p</i> value
DCI-MRI parameters	Ktrans (min <sup>-1</sup> )	NP + Rh-endostatin	0.60 ± 0.94	0.24 ± 0.43	0.02
		NP + Placebo	2.51 ± 5.55	2.40 ± 5.02	0.65
	Kep (min <sup>-1</sup> )	NP + Rh-endostatin	1.08 ± 1.17	0.87 ± 1.21	0.56
		NP + Placebo	2.94 ± 5.22	2.01 ± 2.92	0.46
	Ve	NP + Rh-endostatin	1.06 ± 2.24	0.83 ± 0.95	0.64
		NP + Placebo	2.55 ± 3.66	0.81 ± 0.50	0.27
Bone metabolites	PINP (ng/mL)	NP + Rh-endostatin	327.47 ± 431.04	330.24 ± 395.65	0.08
		NP + Placebo	71.08 ± 32.97	74.16 ± 37.11	0.87
	CTX (ng/L)	NP + Rh-endostatin	1369.5 ± 1347.0	1320.7 ± 1188.9	0.78
		NP + Placebo	551.60 ± 68.53	397.80 ± 332.80	0.38
Tumor markers	CEA (ng/mL)	NP + Rh-endostatin	331.97 ± 587.10	309.53 ± 508.30	0.55
		NP + Placebo	453.01 ± 502.44	706.33 ± 277.34	0.22
	CA125 (U/mL)	NP + Rh-endostatin	50.15 ± 37.18	38.90 ± 22.87	0.47
		NP + Placebo	58.88 ± 37.65	49.88 ± 31.55	0.60
Vascular growth related genes	VEGF (pg/ml)	NP + Rh-endostatin	166.58 ± 127.74	192.18 ± 127.11	0.70
		NP + Placebo	723.82 ± 107.28	688.26 ± 200.3	0.72

than patients with a decrease of  $\leq 50\%$  ( $P = 0.026$ ; **Figure 4A**). A decrease of  $> 50\%$  in the Ktrans value was associated with a median PFS of 6.25 months. The median PFS was 6.15 months when the decrease in Ktrans was  $\leq 50\%$ . The difference in PFS between the 2 groups was not statistically significant ( $P > 0.05$ ; **Figure 4B**).

The “partial remission plus stable disease (PR + SD)” group was defined as group A, and the

disease progression (PD) group was defined as group B. In group A ( $n = 20$ ), the Ktrans value decreased from  $1.29 \pm 3.28/\text{min}$  at baseline to  $0.96 \pm 2.96/\text{min}$  ( $P = 0.03$ ). In group B ( $n = 8$ ), the Ktrans value decreased from  $0.33 \pm 0.33/\text{min}$  to  $0.20 \pm 0.25/\text{min}$  ( $P = 0.44$ ; **Figure 5**).

### Discussion

The concept of precision medicine is that individual variability should be taken into account

## DCE-MRI in the prediction of endostatin effect in NSCLC patients with BM

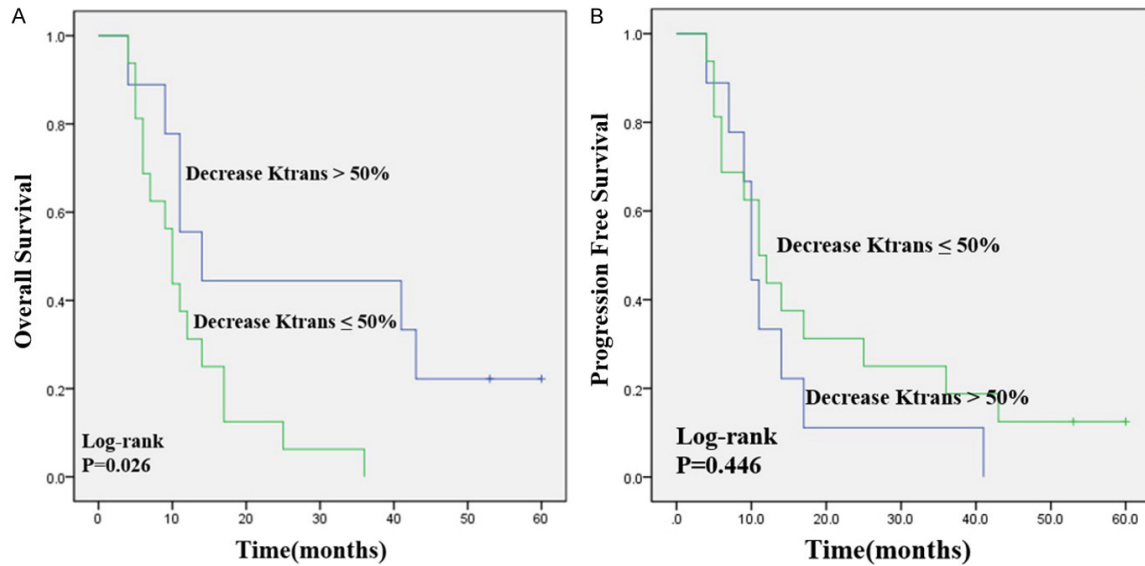


**Figure 4.** PFS and OS between the decreased Ktrans > 50% group and the decreased Ktrans ≤ 50% group. A: The OS between the two groups ( $P = 0.026$ ). B: The PFS in the two groups ( $P = 0.446$ ).

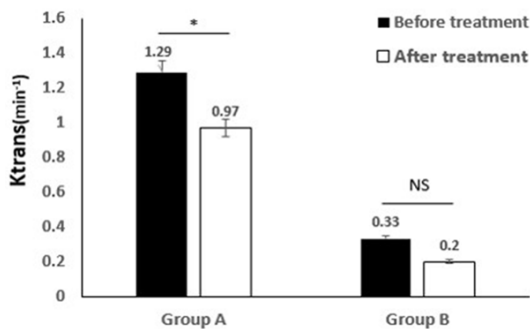


**Figure 5.** Ktrans change of group A and group B before and after treatment. Before and after treatment the changes of Ktrans in the group A were significantly different. \* $P < 0.05$ . NS, non-significant.

when considering disease prevention and treatment strategies. Individualized medicine is an important component of precision medicine. Accurate assessment of treatment effects is needed to better guide subsequent therapies. DCE-MRI quantitative analysis technology can provide accurate individualized therapeutic evaluation for patients. It can accurately evaluate the therapeutic effect in BM lesions, as well as the efficacy of anti-angiogenic therapy.

BM are typically located in irregularly shaped bones and are difficult to measure with rulers. The RECIST guidelines, updated at the end of 2008, define most BM as unmeasurable lesions [23]. Therefore, the therapeutic response of BM lesions is difficult to precisely assess.

Many studies have used DCE-MRI qualitative analysis methods to accurately evaluate the therapeutic response of malignancies [24–26]. However, only a few research studies have used it to evaluate the effect of treatment on BM lesions. Therefore, we investigated the possibility of applying the technology to BM lesions. With DCE-MRI, a series of quantitative parameters such as Ktrans, Kep, and Ve, which could reflect blood perfusion and be used to evaluate the physiological characteristics of tumor blood vessels, were obtained using a two-compartment model. Bäuerle et al found that amplitude and Kep decreased significantly after administration of zoledronic acid and sunitinib malate monotherapy for treatment of bone metastases [27]. In our study, when the enrolled patients were divided into groups A and B according to the RECIST guidelines, we found that the Ktrans value in group A significantly decreased after the treatment, but was not significantly different from that in group B. This may indicate that decreased Ktrans reflects treatment efficacy in BM lesions.

Some previous studies also showed that DCE-MRI quantitative parameters can predict the prognosis of NSCLC patients with BM. For instance, in metastatic renal carcinoma and colorectal liver metastases, a higher baseline Ktrans value and a significant reduction in the Ktrans value after treatment were associated with better PFS [28, 29]. However, studies on

## DCE-MRI in the prediction of endostatin effect in NSCLC patients with BM

**Table 4.** Comparison of adverse reaction rate between two groups

Group	Treatment group (n = 22)	Incidence rate (%)	Control group (n = 11)	Incidence rate (%)	P value
Myelosuppression	8	36.4	4	36.4	> 0.05
First or Second degree	6	27.3	3	27.3	> 0.05
Third or fourth degree	2	9.1	1	9.1	> 0.05
Nausea and Vomiting	9	40.9	4	36.4	> 0.05
Liver disfunction	7	31.8	3	27.3	> 0.05
Renal disfunction	2	9.1	1	9.1	> 0.05
ECG ST-T change	1	4.5	0	0.00	> 0.05
Anemia	2	9.1	1	9.1	> 0.05
Neurotoxicity	1	4.5	0	0.00	> 0.05
Hypertension	0	0.0	0	0.00	> 0.05
Thrombosis	0	0.0	0	0.00	> 0.05

The incidence of adverse reaction rate was not statistically different between the two groups ( $P > 0.05$ ).

lung cancer are relatively limited. In our study, we found that patients with a decrease of > 50% in the Ktrans value had a longer OS, which demonstrated that the Ktrans may correlate with the prognosis of NSCLC patients with BM to some extent.

DCE-MRI is a reproducible, noninvasive technique to evaluate tumor vascularization [30]. DCE-MRI quantitative analysis technology can reflect the treatment effect through changes in quantitative parameters. Thus, we aimed to precisely evaluate the therapeutic response and predict the early efficacy of anti-angiogenic therapy in NSCLC patients with BM using DCE-MRI.

The efficacy of rh-endostatin has been previously confirmed in many clinical trials. Rh-endostatin with chemotherapy attained a higher tumor response rate without increasing toxicity in breast cancer patients and can significantly prolong the survival time of postoperative NSCLC patients [31, 32]. In our clinical trial, we found that the ORR in the treatment group was 30% (6/18), compared with 0% in the control group, suggesting that rh-endostatin could synergize the antitumor effect of vinorelbine- and cisplatin-based chemotherapy in NSCLC patients with BM. However, the difference in DCR between the 2 groups was not significant. This is mainly because most of the patients in the treatment or control group achieved SD. The OS in the treatment group was significantly longer than that in the control group. This may

be because the treatment group included 2 patients who subsequently underwent targeted therapy for EGFR mutations. Initial studies of NSCLC indicated improved response rates and prognosis in patients expressing or overexpressing EGFR [33]. Both of these patients had a longer survival time than the others. Moreover, no significant difference in the incidence of adverse reactions was found between the 2 groups (Table 4).

The current criteria for evaluating anti-angiogenic efficacy are insufficient, as

tumor shrinkage occurs after blood perfusion decreases [34]. DCE-MRI quantitative parameters have also been used widely in many clinical trials to precisely evaluate the early effects of anti-angiogenic therapy. For example, a murine xenograft model of human lung cancer was used to evaluate in vivo vascular functions, and in locally advanced breast cancer patients, the DCE-MRI quantitative analysis method was used to evaluate the anti-angiogenic and anti-tumor effects of rh-endostatin combined with docetaxel and epirubicin [35, 36]. In our study, the decrease in Ktrans value in the treatment group ( $P = 0.02$ ) was significantly greater than that in the control group ( $P = 0.65$ ). Thus, we believe that Ktrans can be used to evaluate the efficacy of early anti-angiogenic therapy.

Bevacizumab is an internationally accepted first-line anti-angiogenic drug, and its anti-angiogenic effect has been confirmed in many clinical trials [37, 38]. In China, rh-endostatin has been widely used in patients with stage IV NSCLC [39, 40]. It has several anti-angiogenic mechanisms [41, 42]. Vascular endothelial growth factor-2 (VEGF-2) is a known endothelial target expressed in NSCLC tumor cells [43]. Rh-endostatin can play a major antiangiogenic role by specifically acting on VEGF-2 of tumor-associated neovascular endothelial cells, inhibiting cell migration, and inducing cell apoptosis.

However, in this study, the values of the DCE-MRI quantitative parameters Kep and Ve, bone



metabolism, values of the tumor markers, and expression levels of angiogenesis-related genes in serum were not significantly different before and after treatment in the 2 groups, which suggests that they lack sensitivity to evaluate the therapeutic response in the NSCLC patients with BM. These results may be due to the limited number of patients enrolled in our study. Larger clinical trials are required to validate whether or not a relationship exists between the changes in these indicators and the response of BM lesions to antivasular treatment.

The limitations of this study should be considered, including its relatively small number of patients and the fact that it is a single-center clinical study. Thus, more multicenter clinical trials are needed to further confirm our study results. We will also apply this approach to other anti-angiogenic drugs for further verification of whether DCE-MRI can be used to assess early anti-angiogenic effects and the therapeutic response of BM lesions.

### Conclusion

The DCE-MRI quantitative parameter *K*<sub>trans</sub> could be used to precisely evaluate the therapeutic response of BM lesions after anti-angiogenic therapy and predict patient survival. Therefore, we believe that DCE-MRI quantitative analysis technology might have broad applications in the field of precision medicine. Moreover, we reconfirmed that rh-endostatin could improve the treatment response in NSCLC patients with BM.

### Acknowledgements

We acknowledge that the study was supported by the National Natural Science Foundation of China (grant No. 81201628).

### Disclosure of conflict of interest

None.

### Abbreviations

BM, bone metastasis; DCE-MRI, dynamic contrast-enhanced magnetic resonance imaging; NSCLC, non-small-cell lung cancer; NP, vinorelbine + cisplatin; CT, chest computed tomography; ORR, objective response rate; DCR, dis-

ease control rate; PR, partial remission; SD, stable disease; PD, disease progression; WHO, World Health Organization; RECIST, Response Evaluation Criteria in Solid Tumors; MRI, magnetic resonance imaging; *K*<sub>trans</sub>, volume of transport constant; *K*<sub>ep</sub>, rate constant; *V*<sub>e</sub>, extravascular extracellular volume fraction; OS, overall survival; PFS, progression-free survival; FSE T1WI, fast spin-echo T1-weighted image; FSE T2WI, fast spin-echo T2-weighted image; ROI, region of interest; EGFR, epidermal growth factor receptor; VEGF, vascular endothelial growth factor; VEGFR-2, vascular endothelial growth factor 2.

**Address correspondence to:** Hui Zhao, Department of Internal Oncology, Shanghai Sixth People's Hospital Affiliated to Shanghai Jiaotong University, Shanghai 200233, People's Republic of China. E-mail: zhao-hui@sjtu.edu.cn

### References

- [1] Wang J, Wang K, Xu J, Huang J, Zhang T. Prognostic significance of circulating tumor cells in non-small-cell lung cancer patients: a meta-analysis. *PLoS One* 2013; 8: e78070.
- [2] Rossi A, Chiodini P, Sun JM, O'Brien ME, von Plessen C, Barata F, Park K, Popat S, Bergman B, Parente B, Gallo C, Gridelli C, Perrone F, Di Maio M. Six versus fewer planned cycles of first-line platinum-based chemotherapy for non-small-cell lung cancer: a systematic review and meta-analysis of individual patient data. *Lancet Oncol* 2014; 15: 1254-62.
- [3] Sun JM, Ahn JS, Lee S, Kim JA, Lee J, Park YH. Predictors of skeletal-related events in non-small cell lung cancer patients with bone metastases. *Lung Cancer* 2011; 71: 89-93.
- [4] Lopez-Olivo MA, Shah NA, Pratt G, Risser JM, Symanski E, Suarez-Almazor ME. Bisphosphonates in the treatment of patients with lung cancer and metastatic bone disease: a systematic review and meta-analysis. *Support Care Cancer* 2012; 20: 2985-98.
- [5] Bauerle T, Semmler W. Imaging response to systemic therapy for bone metastases. *Eur Radiol* 2009; 19: 2495-507.
- [6] Eisenhauer EA, Therasse P, Bogaerts J, Schwartz LH, Sargent D, Ford R, Dancey J, Arbuck S, Gwyther S, Mooney M, Rubinstein L, Shankar L, Dodd L, Kaplan R, Lacombe D, Verweij J. New response evaluation criteria in solid tumours: revised RECIST guideline (version 1.1). *Eur J Cancer (Oxford, England: 1990)* 2009; 45: 228-47.

- [7] Hollingsworth SJ. Precision medicine in oncology drug development: a pharma perspective. *Drug Discov Today* 2015; 20: 1455-63.
- [8] Wijesinghe P, Bollig-Fischer A. Lung cancer genomics in the Era of accelerated targeted drug development. *Adv Exp Med Biol* 2016; 890: 1-23.
- [9] Ma W, Xu M, Liu Y, Liu H, Huang J, Zhu Y, Ji LJ, Qi X. Safety profile of combined therapy inhibiting EFGR and VEGF pathways in patients with advanced non-small-cell lung cancer: a meta-analysis of 15 phase II/III randomized trials. *Int J Cancer* 2015; 137: 409-19.
- [10] Fiorio Pla A, Munaron L. Functional properties of ion channels and transporters in tumour vascularization. *Philos Trans R Soc Lond B Biol Sci* 2014; 369: 20130103.
- [11] Rong B, Yang S, Li W, Zhang W, Ming Z. Systematic review and meta-analysis of endostar (rh-endostatin) combined with chemotherapy versus chemotherapy alone for treating advanced non-small cell lung cancer. *World J Surg Oncol* 2012; 10: 170-82.
- [12] Liu G, Rugo HS, Wilding G, McShane TM, Evelhoch JL, Ng C, Jackson E, Kelcz F, Yeh BM, Lee FT Jr, Charnsangavej C, Park JW, Ashton EA, Steinfeldt HM, Pithavala YK, Reich SD, Herbst RS. Dynamic contrast-enhanced magnetic resonance imaging as a pharmacodynamic measure of response after acute dosing of AG-013736, an oral angiogenesis inhibitor, in patients with advanced solid tumors: results from a phase I study. *J Clin Oncol* 2005; 23: 5464-73.
- [13] Bauerle T, Bartling S, Berger M, Schmitt-Gräff A, Hilbig H, Kauczor HU, Delorme S, Kiessling F. Imaging anti-angiogenic treatment response with DCE-VCT, DCE-MRI and DWI in an animal model of breast cancer bone metastasis. *Eur J Radiol* 2010; 73: 280-7.
- [14] Chang YC, Yu CJ, Chen CM, Hu FC, Hsu HH, Tseng WY, Ting-Fang Shih T, Yang PC, Chih-Hsin Yang J. Dynamic contrast-enhanced MRI in advanced nonsmall-cell lung cancer patients treated with first-line bevacizumab, gemcitabine, and cisplatin. *J Magn Reson Imaging* 2012; 36: 387-96.
- [15] Collins FS, Varmus H. A new initiative on precision medicine. *N Engl J Med* 2015; 372: 793-5.
- [16] Zheng D, Chen Y, Chen Y, Xu LX, Chen WB, Yao Y, Du Z, Deng X, Chan Q. Dynamic contrast-enhanced MRI of nasopharyngeal carcinoma: a preliminary study of the correlations between quantitative parameters and clinical stage. *J Magn Reson Imaging* 2014; 39: 940-8.
- [17] Yeo DM, Oh SN, Jung CK, Lee MA, Oh ST, Rha SE, Jung SE, Byun JY, Gall P, Son Y. Correlation of dynamic contrast-enhanced MRI perfusion parameters with angiogenesis and biologic aggressiveness of rectal cancer: preliminary results. *J Magn Reson Imaging* 2015; 41: 474-80.
- [18] Tofts PS, Brix G, Buckley DL, Evelhoch JL, Henderson E, Knopp MV, Larsson HB, Lee TY, Mayr NA, Parker GJ, Port RE, Taylor J, Weisskoff RM. Estimating kinetic parameters from dynamic contrast-enhanced T(1)-weighted MRI of a diffusible tracer: standardized quantities and symbols. *J Magn Reson Imaging* 1999; 10: 223-32.
- [19] Yang JF, Zhao ZH, Zhang Y, Zhao L, Yang LM, Zhang MM, Wang BY, Wang T, Lu BC. Dual-input two-compartment pharmacokinetic model of dynamic contrast-enhanced magnetic resonance imaging in hepatocellular carcinoma. *World J Gastroenterol* 2016; 22: 3652-62.
- [20] Pickles MD, Lowry M, Manton DJ, Gibbs P, Turnbull LW. Role of dynamic contrast enhanced MRI in monitoring early response of locally advanced breast cancer to neoadjuvant chemotherapy. *Breast Cancer Res Treat* 2005; 91: 1-10.
- [21] Takahashi T, Kalka C, Masuda H, Chen D, Silver M, Kearney M, Magner M, Isner JM, Asahara T. Ischemia- and cytokine-induced mobilization of bone marrow-derived endothelial progenitor cells for neovascularization. *Nat Med* 1999; 5: 434-8.
- [22] Tetreault MP, Weinblatt D, Ciolino JD, Kleinszanto AJ, Sackey BK, Twyman-Saint Victor C, Karakasheva T, Teal V, Katz JP. Esophageal expression of active IkappaB kinase-beta in mice up-regulates tumor necrosis factor and granulocyte-macrophage colony-stimulating factor, promoting inflammation and angiogenesis. *Gastroenterology* 2016; 150: 1609-19, e11.
- [23] Costelloe CM, Chuang H, Madewell JE, Ueno NT. Cancer response criteria and bone metastases: RECIST 1.1, MDA and PERCIST. *J Cancer* 2010; 1: 80-92.
- [24] Zheng D, Chen Y, Chen Y, Xu L, Ren W, Chen W, Chan Q. Early response to chemoradiotherapy for nasopharyngeal carcinoma treatment: value of dynamic contrast-enhanced 3.0 T MRI. *J Magn Reson Imaging* 2015; 41: 1528-40.
- [25] Nguyen HT, Jia G, Shah ZK, Pohar K, Mortazavi A, Zynger DL, Wei L, Yang X, Clark D, Knopp MV. Prediction of chemotherapeutic response in bladder cancer using K-means clustering of dynamic contrast-enhanced (DCE)-MRI pharmacokinetic parameters. *J Magn Reson Imaging* 2015; 41: 1374-82.
- [26] Li X, Arlinghaus LR, Ayers GD, Chakravarthy AB, Abramson RG, Abramson VG, Atuegwu N, Farley J, Mayer IA, Kelley MC, Meszoely IM, Means-Powell J, Grau AM, Sanders M, Bhave SR, Yankeeelov TE. DCE-MRI analysis methods for predicting the response of breast cancer to

- neoadjuvant chemotherapy: pilot study findings. *Magn Reson Med* 2014; 71: 1592-602.
- [27] Bauerle T, Merz M, Komljenovic D, Zwick S, Semmler W. Drug-induced vessel remodeling in bone metastases as assessed by dynamic contrast enhanced magnetic resonance imaging and vessel size imaging: a longitudinal in vivo study. *Clin Cancer Res* 2010; 16: 3215-25.
- [28] Hahn OM, Yang C, Medved M, Karczmar G, Kistner E, Karrison T, Manchen E, Mitchell M, Ratain MJ, Stadler WM. Dynamic contrast-enhanced magnetic resonance imaging pharmacodynamic biomarker study of sorafenib in metastatic renal carcinoma. *J Clin Oncol* 2008; 26: 4572-8.
- [29] De Bruyne S, Van Damme N, Smeets P, Ferdinande L, Ceelen W, Mertens J, Van de Wiele C, Troisi R, Libbrecht L, Laurent S, Geboes K, Peeters M. Value of DCE-MRI and FDG-PET/CT in the prediction of response to preoperative chemotherapy with bevacizumab for colorectal liver metastases. *Br J Cancer* 2012; 106: 1926-33.
- [30] Panebianco V, Iacovelli R, Barchetti F, Altavilla A, Forte V, Sciarra A, Cortesi E, Catalano C. Dynamic contrast-enhanced magnetic resonance imaging in the early evaluation of anti-angiogenic therapy in metastatic renal cell carcinoma. *Anticancer Res* 2013; 33: 5663-6.
- [31] Chen J, Yao Q, Li D, Zhang J, Wang T, Yu M, Zhou X, Huan Y, Wang J, Wang L. Neoadjuvant rh-endostatin, docetaxel and epirubicin for breast cancer: efficacy and safety in a prospective, randomized, phase II study. *BMC Cancer* 2013; 13: 248-55.
- [32] Zhu Q, Zang Q, Jiang ZM, Wang W, Cao M, Su GZ, Zhen TC, Zhang XT, Sun NB, Zhao C. Clinical application of recombinant human endostatin in postoperative early complementary therapy on patients with non-small cell lung cancer in Chinese mainland. *Asian Pac J Cancer Prev* 2015; 16: 4013-8.
- [33] Dahabreh IJ, Linardou H, Kosmidis P, Bafaloukos D, Murray S. EGFR gene copy number as a predictive biomarker for patients receiving tyrosine kinase inhibitor treatment: a systematic review and meta-analysis in non-small-cell lung cancer. *Ann Oncol* 2011; 22: 545-52.
- [34] Huang C, Wang X, Wang J, Lin L, Liu Z, Xu W, Wang L, Xiao J, Li K. Incidence and clinical implication of tumor cavitation in patients with advanced non-small cell lung cancer induced by Endostar, an angiogenesis inhibitor. *Thorac Cancer* 2014; 5: 438-46.
- [35] Yuan A, Lin CY, Chou CH, Shih CM, Chen CY, Cheng HW, Chen YF, Chen JJ, Chen JH, Yang PC, Chang C. Functional and structural characteristics of tumor angiogenesis in lung cancers overexpressing different VEGF isoforms assessed by DCE- and SSCE-MRI. *PLoS One* 2011; 6: e16062.
- [36] Jia Q, Xu J, Jiang W, Zheng M, Wei M, Chen J, Wang L, Huan Y. Dynamic contrast-enhanced MR imaging in a phase study on neoadjuvant chemotherapy combining rh-endostatin with docetaxel and epirubicin for locally advanced breast cancer. *Int J Med Sci* 2013; 10: 110-8.
- [37] Herbst RS, Ansari R, Bustin F, Flynn P, Hart L, Otterson GA, Vlahovic G, Soh CH, O'Connor P, Hainsworth J. Efficacy of bevacizumab plus erlotinib versus erlotinib alone in advanced non-small-cell lung cancer after failure of standard first-line chemotherapy (BeTa): a double-blind, placebo-controlled, phase 3 trial. *Lancet (London, England)* 2011; 377: 1846-54.
- [38] Niho S, Kunitoh H, Nokihara H, Horai T, Ichinose Y, Hida T, Ichinose Y, Hida T, Yamamoto N, Kawahara M, Shinkai T, Nakagawa K, Matsui K, Negoro S, Yokoyama A, Kudoh S, Kiura K, Mori K, Okamoto H, Sakai H, Takeda K, Yokota S, Saijo N, Fukuoka M. Randomized phase II study of first-line carboplatin-paclitaxel with or without bevacizumab in Japanese patients with advanced non-squamous non-small-cell lung cancer. *Lung Cancer* 2012; 76: 362-7.
- [39] Zhao X, Mei K, Cai X, Chen J, Yu J, Zhou C, Li Q. A randomized phase II study of recombinant human endostatin plus gemcitabine/cisplatin compared with gemcitabine/cisplatin alone as first-line therapy in advanced non-small-cell lung cancer. *Invest New Drugs* 2012; 30: 1144-9.
- [40] Liu ZJ, Wang J, Wei XY, Chen P, Wang LC, Lin L, Sun BC, Li K. Predictive value of circulating endothelial cells for efficacy of chemotherapy with rh-endostatin in non-small cell lung cancer. *J Cancer Res Clin Oncol* 2012; 138: 927-37.
- [41] Han B, Xiu Q, Wang H, Shen J, Gu A, Luo Y, Bai C, Guo S, Liu W, Zhuang Z, Zhang Y, Zhao Y, Jiang L, Zhou J, Jin X. A multicenter, randomized, double-blind, placebo-controlled study to evaluate the efficacy of paclitaxel-carboplatin alone or with endostar for advanced non-small cell lung cancer. *J Thorac Oncol* 2011; 6: 1104-9.
- [42] Sato Y. Persistent vascular normalization as an alternative goal of anti-angiogenic cancer therapy. *Cancer Sci* 2011; 102: 1253-6.
- [43] Yang F, Tang X, Riquelme E, Behrens C, Nilsson MB, Giri U, Varella-Garcia M, Byers LA, Lin HY, Wang J, Raso MG, Girard L, Coombes K, Lee JJ, Herbst RS, Minna JD, Heymach JV, Wistuba II. Increased VEGFR-2 gene copy is associated with chemoresistance and shorter survival in patients with non-small-cell lung carcinoma who receive adjuvant chemotherapy. *Cancer Res* 2011; 71: 5512-21.